Workshop 4A: Identifying and mapping landforms and quantifying fault displacement with lidar digital topographic data

Leaders: Kurt Frankel (Georgia Tech) and Ramon Arrowsmith (ASU)

Introduction

Any successful study of tectonics and topography must begin with a detailed analysis of the landscape. A key component to many recent fault system investigations airborne lidar digital topographic data. These data facilitate the efficient identification, mapping, and analysis of deformed landforms in unprecedented detail (e.g., Carter et al., 2007; Hudnut et al., 2002; Arrowsmith and Zielke, 2009; Frankel et al., 2007a,b; Oskin et al., 2007). Lidar data have several great advantages over previously available forms of remotely-sensed and digital topographic data. In particular, surveying of deformed geomorphic features (e.g., offset channels and alluvial fans) and the construction of high precision topographic maps, which would take days to weeks with traditional surveying methods, can be accomplished in minutes with lidar data.

Moreover, the high-resolution topographic data can be digitally manipulated to enhance and reveal subtle topographic features, something not possible with most aerial photographs, satellite imagery, or lower-resolution digital elevation data. For example, the landscape can be artificially illuminated from any angle to highlight previously unrecognized features of the landscape and surface slope and slope aspect maps can also be easily constructed to reveal and retrodeform subtle topographic features (e.g., Frankel, 2007; Frankel et al., 2007a,b; Oskin et al., 2007; Arrowsmith and Zielke, 2010; Zielke et al., 2010). Furthermore, this technology holds the ability to "see through" canopies in vegetated regions, thus revealing an image of the "bare earth" beneath the trees and illuminating landscapes that could not previously be investigated in detail with aerial photographs or other forms of remotely-sensed images (e.g., Carter et al., 2007; Prentice et al., 2009). These data can also be used to more objectively map and quantify the evolution of alluvial landforms through time by developing various algorithms to measure surface roughness characteristics (e.g., Frankel and Dolan, 2007; McKean and Roering, 2004; Glenn et al., 2006). By combining detailed landform analyses from lidar data with age control from improved Quaternary geochronometers researchers are gaining unprecedented insight into the rates and patterns of lithospheric deformation and landscape evolution.

Objectives

This workshop will cover the basics of alluvial fan mapping and quantifying fault displacement using airborne lidar data. Exercises will focus on strike-slip fault systems, although many of the principles apply to other deformational regimes. We will start with a qualitative mapping exercise that uses diagnostic morphologic characteristics to define alluvial fan units and fault traces. Next, participants will produce slope and surface roughness maps derived from lidar data for comparison with the more standard (and qualitative) geologic map (e.g., Frankel and Dolan, 2007).

Following the mapping exercises, fault displacements will be quantified on the basis of channel morphology (e.g., Zielke et al., 2010), using the LaDiCaoz (Matlab-based) tools developed by Olaf Zielke.

Study Areas

Death Valley

We will use an example from northern Death Valley for the alluvial fan and fault mapping exercise. Death Valley is located along the western edge of the Great Basin, at the transition between the extensional Basin and Range Province and the strike-slip faults comprising the eastern California shear zone (Figure 1). Death Valley is a pull-apart basin formed by a step-over between the right-lateral southern Death Valley and northern Death Valley fault zones. Displacement along a down-to-the-west normal fault forms the deep, central basin between the two strike-slip fault systems (Burchfiel and Stewart, 1966). Opening of the basin as a result of continued tectonic activity since at least the Miocene has produced the accommodation space necessary for continuous deposition of alluvial deposits (Hamilton, 1988; Wernicke et al., 1988; Burchfiel et al., 1995). Rates of tectonic activity range from 1 to 3 mm/yr along the normal fault in central Death Valley to ~4.5 mm/yr on the northern Death Valley fault zone (Brogan et al., 1991; Klinger, 2001; Knott et al., 2002; Frankel et al., 2007).

Climate in the region during late-Pleistocene and Holocene time has been dominated by two wet, cold periods and two warm, dry intervals (Li et al., 1996; Lowenstein et al., 1999). Perennial lakes existed in the central basin during the penultimate glacial advance from ~128 to 186 ka (oxygen isotope stage 6) and the last glacial maximum from ~12 to 35 ka (oxygen isotope stage 2) when the climate was cooler and wetter (Lowenstein et al., 1999). From 60 to 120 ka, climate is thought to have been similar to the aridity characterizing the Holocene environment (Lowenstein et al., 1999). The period from 35 to 60 ka was a time of unstable climate and hence, fluctuating lake levels. The present-day arid climate results from the large rain shadow produced by the Sierra Nevada, Inyo Mountains, and Panamint Mountains (Poage and Chamberlin, 2002). With elevations up to ~4400 m, these three ranges inhibit the eastward migration of moist air masses coming from the Pacific Ocean. As a result, modern-day precipitation in central Death Valley is a sparse ~6 cm/yr (Western Region Climate Center - http://www.wrcc.dri.edu).

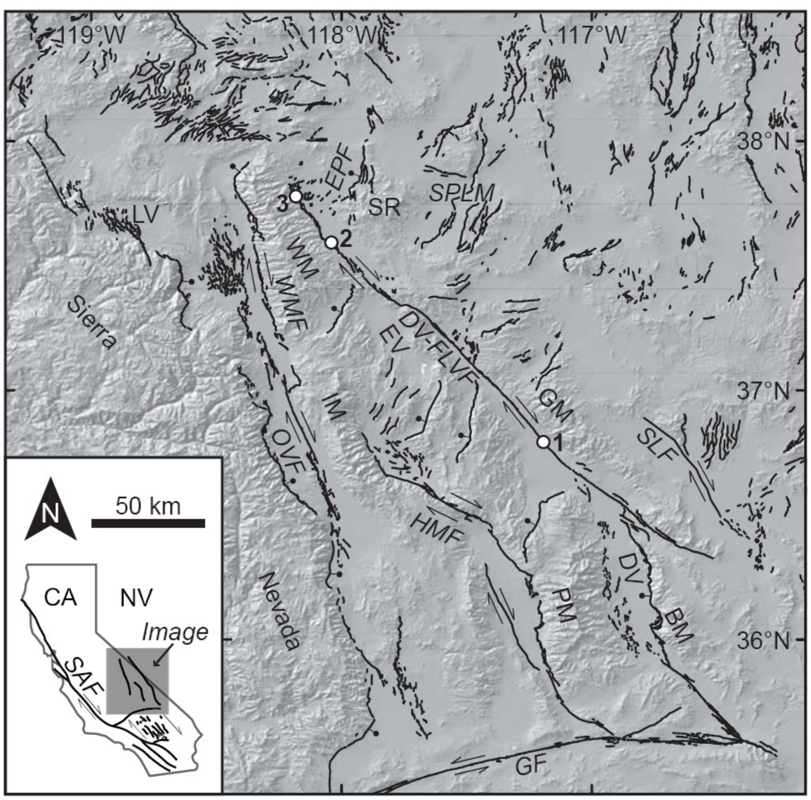

Figure 1. Location map of the Death Valley study area. LV = Long Valley Caldera, WM = White Mountains, DV = Death Valley, BM = Black Mountains, DV-FLVF = Death Valley-Fish Lake Valley fault, PM = Panamint Mountains, GF = Garlock fault, OVF = Owens Valley fault, WMF = White Mountains fault, EV = Eureka Valley, SLF = Stateline fault, GM = Grapevine Mountains, SR = Silver Peak Range, HMF = Hunter Mountain fault. Location 1 is the Red Wall Canyon alluvial fan, which is used as a case study for this short course.

San Andreas Fault—Carrizo Plain

Surface slip reconstructions of past earthquakes serve to formulate conceptual models for the recurrence of earthquakes along faults. One of the most influential reconstructions was made for the 1857 earthquake and preceding earthquakes along its surface rupture trace on the south-central San Andreas Fault (SAF). It became a cornerstone in the formulation of the characteristic earthquake and uniform slip models which are now widely applied in seismic hazard analysis and earthquake forecasts. The Carrizo section, a ~60km long section of the south-central SAF, plays a critical role in current understanding of recurrence of large earthquakes along the 1857 rupture trace and therefore hazard assessment for southern California. Offset channels along the San Andreas Fault are spectacular and have been noticed for more than 100 years (see discussion in Lawson, 1908). The Carrizo section was thought to experience the largest slip during 1857 and previous large earthquakes (8-10 m), thus controlling the recurrence of 1857-like ruptures with average recurrence times of 250-450 years. Recent work along the south-central SAF has suggested that slip during the 1857 Fort Tejon earthquake along the Carrizo section was 5-6 m (Zielke, et al., 2010), significantly lower than the previously reported 8-10 m, revising a key portion of the data upon which current conceptual models for earthquake recurrence and seismic hazard of southern California are built. Based on these new results, surface rupture along the Carrizo section is thought to be more frequent (less than 150 years recurrence time) and have more variable slip (not all events experienced 5-6 m of slip).

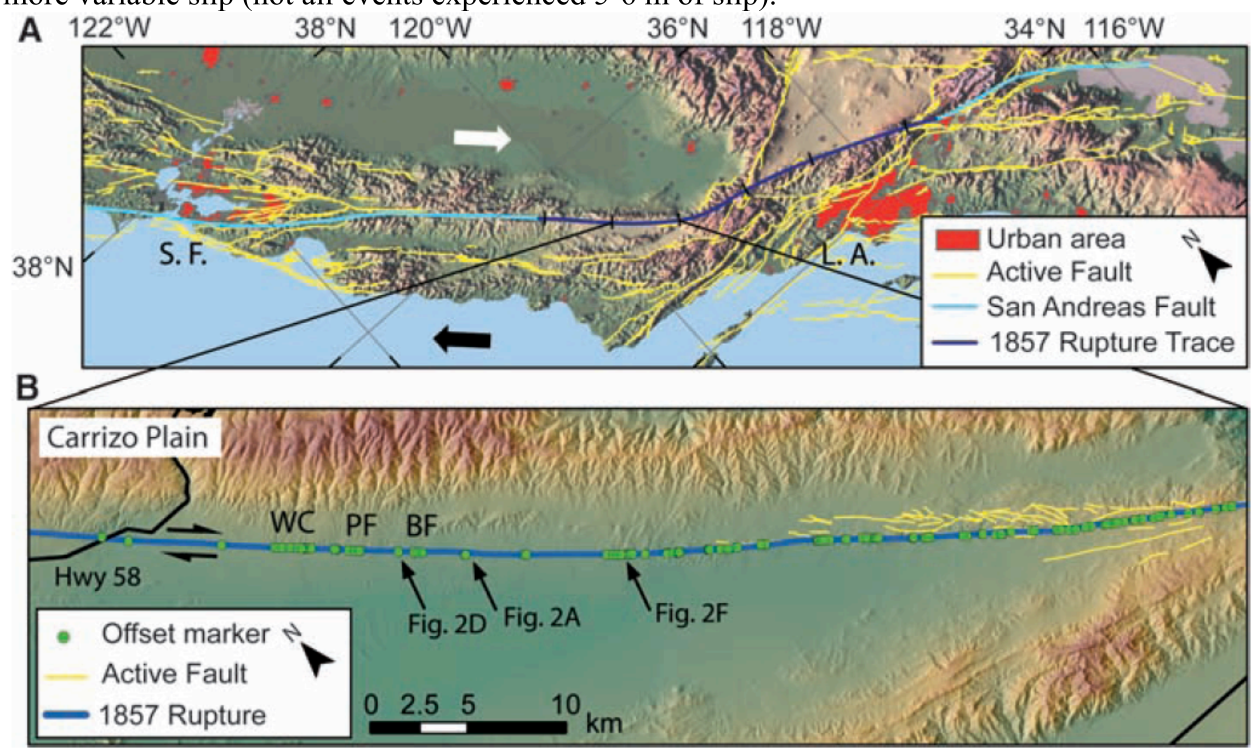

Figure 2. A) Active faults of Southern California along with major population centers. B) Active fault traces and rupture zone of 1857 earthquake in the Carrizo Plain. Site indicate by 2D is the "Sieh31" locality (Sieh, 1978) which is the first target of workshop exercises. From Zielke, et al., 2010.

Alluvial Fan and Fault Mapping

Qualitative Mapping

Alluvial fans are pervasive piedmont features at the base many major mountain ranges. Previous work, both in Death Valley and throughout southwestern North America, has defined a consistent alluvial fan stratigraphy for the region (Denny, 1965; Hunt and Mabey, 1966; Moring, 1986; Bull, 1991; Klinger, 2001). Alluvial fans in our Death Valley study area comprise six distinct lithostratigraphic units - Q4b, Q4a, Q3c, Q3b, Q3a, and Q2c. Unit Q4b represents active alluvial channels and occupies the lowest topographic position in the landscape. Unit Q2c is the oldest alluvial landform in the study area and thus stands topographically higher than the other units (Fig. 3). In a general sense, the units are broken out in terms of qualitative metrics such as bar and swale morphology and varnish and soil development. Detailed descriptions of the alluvial fan stratigraphy can be found in the Bull (1991). Although the most detailed maps are best compiled in the field, many of these fan units can be mapped to a first order from lidar topographic data based on their geomorphic characteristics.

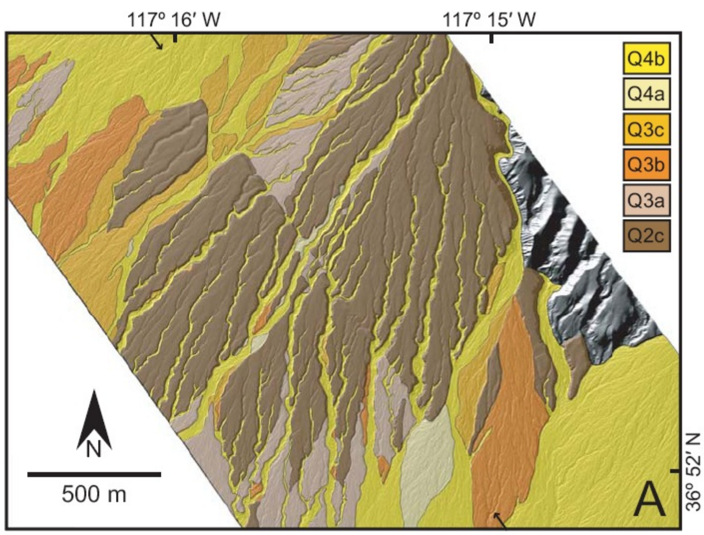

Figure 3. Geologic map of the Red Wall Canyon alluvial fan in northern Death Valley. Arrows indicate trace of the northern Death Valley fault. Modified from Frankel and Dolan (2007) and Klinger (2001).

The first thing you'll want to do for mapping landforms is construct a hillshade image from the lidar-derived DEM. Once the DEM is loaded in ArcMap, do the following:

1. Enter ArcToolbox
   navigate to 3D Analyst Tools → Raster Surface → Hillshade

2. Select your input dataset (Input raster)

3. Define the name for your hillshade image

4. Define the azimuth and altitude for the sun angle (optional – default is 315° and 45°)

5. Click OK

You should now have a hillshade image, which will greatly enhance your ability to map different alluvial fan units, which will look something like Figure 4.

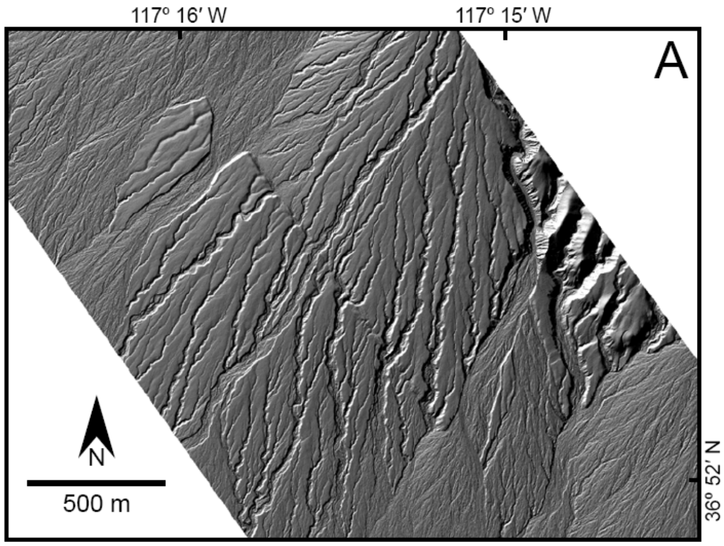

Figure 4. Hillshaded lidar-derived DEM of the the Red Wall Canyon alluvial fan in northern Death Valley. After Frankel and Dolan (2007).

Next, you will want to make shape files for your faults and map units. To do this, first open ArcCatalog and then proceed as follows.

1. Navigate to the directory where you want your shape file(s) to reside. You will probably want a separate shape file for each component of your map (i.e., faults, individual units, etc.).

2. Right-click under the “Contents” tab and choose New → Folder to make a folder where your shape files will reside.

3. Right-click on your new folder and choose New → Shapefile

4. You will now be prompted to enter information about the coordinate system and projection of the shape file. These should be the same as the underlying DEM. In the example, this is a UTM projection, NAD83 datum, zone 11N.

5. Make sure you also enter a name for your shape file (either map unit or fault) and select whether that shape file is composed of polygons (for map units) or polylines (for faults). Again, each map unit, fault, etc. should have a separate shape file.

5. Once you have defined the projection and coordinate system, your new shape file will be visible in the ArcCatalog window. From here, drag this into the “Layers” menu on the left side of your ArcMap window. You are now ready to begin mapping this unit.

6. To begin mapping, first map sure your shape file is listed *above* your hillshaded DEM in the Layers menu.

7. Next open the "Editor" toolbar by clicking View → Toolbars → Editor

8. Once the Editor toolbar appears, click Editor → Start Editing
9. At this point, you will be asked which data you want to edit. Select your shape file and click OK.

10. In the Editor toolbar, make sure to select the following
    Task: Create New Feature
    Target: the unit or fault you want to edit

11. Click on the pencil in the Editor toolbar and begin drafting the map units. Double click at the end of your polygon to stop drawing.

12. When you are finished mapping, click Editor → Stop Editing

13. You can now double click on the shape file in the Layers menu to change unit colors, transparency, etc. to clean up your map. Be sure to save these changes! Following these steps should allow you to produce a map similar to Figure 5.

Slope Maps

Slope maps can be extremely useful for indentifying faults, particularly in a low-relief landscape as is common where faults cut alluvial fans. Often, active faults are expressed geomorphically as scarps cutting alluvium. These scarps tend to be significantly steeper than surrounding topography and thus, slope maps often reveal the scarp topography in dramatic fashion (Figure 5). In addition, slope maps can aid in the identification of secondary fault strands and off-fault deformation. To produce a slope map, follow the directions below:

1. Enter ArcToolbox
    navigate to 3D Analyst Tools → Raster Surface → Slope

2. Select your input dataset (Input raster)

3. Define the name for your slope

4. Click "OK"

By default, a "classified" slope map will be produced and displayed. To improve the clarity of the map, you will want to turn this into a "stretched" slope map, which can be displayed by the following.

1. Double click on the slope map title in the "Layers" menu on the left of your screen.

2. Click on the “Symbology” tab.

3. On the left side of the Symbology window, select “Stretched”

4. Select the color ramp you want to use
5. Click OK

Optional:

You may want to display the slope map either as a pseudo-hillshade or “draped” over the hillshaded topography. To do this, you can click on “Use hillshade effect” beneath the color ramp. Alternatively, you can click on the “Display” tab under Layer Properties and make the slope map semi-transparent (~25%). Then, in the Layers window, position the slope map directly on top of the hillshade to produce a 3D effect.

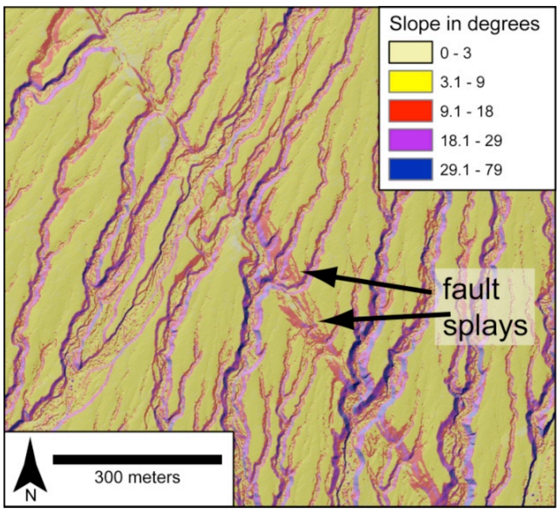

Figure 5. Slope map derived from lidar for the Red Wall Canyon alluvial fan in Death Valley. Image shows the multi-stranded nature of the fault.

Surface Roughness Maps

Surface morphology is one of the most widely used criteria to distinguish alluvial fans of different ages (e.g., Wells et al., 1990; Bull, 1991; Ritter et al., 1993). Previous studies suggest that the relative age of alluvial deposits is manifest by topographic variability, with fan surfaces tending to become smoother with increasing age (Bull, 1977; 1991; Matmon et al., 2006). As a more objective way to map alluvial fan deposits, lidar topographic data can be used to quantify differences in alluvial fan surface roughness, thereby helping identify individual fan units. Although there are many ways in which to measure the texture of alluvial and colluvial material (e.g., McKean and Roering, 2004; Glenn et al., 2006), here surface roughness is defined as the standard deviation of slope. The roughness metric in this way because it allows us to average out surface features over a five-meter by five-meter area, thereby eliminating any anomalies related to individual boulders or the occasional creosote bush. Furthermore, taking this approach to calculating surface roughness accounts more readily for the wavelengths (~5 to 10 m) of typical bar and swale morphology that are commonly observed in arid alluvial environments. For a detailed description of this methodology, please see Frankel (2007) and Frankel and Dolan (2007).

In order to produce a surface roughness map it is easiest to issue the commands for this operation manually using the command line window. Do this via the following steps.

1. Open the command line window by clicking on the “Window” tab on the main ArcMap menu

   Window → Command Line

2. Once the command line window is open, make sure you are in the correct workspace by issuing:

```
workspace c:\workspace
```

   You should now be in the directory where your slope map resides.

3. Now, you will issue the following command to calculate the standard deviation of values in your slope map:

```
FocalStatistics name_slp name_std 3 STD
```

The first part of this command calls the “Focal statistics” tool, which allows for the analysis of values within moving window; the second term – “name_slp” – is the name of your slope map; the third term – “name_std” – is the name of your surface roughness map; the fourth term – “3” – is the cell size of the moving analysis window, which in this case is 3 x 3, or 3 m by 3 m; and the fifth term – “STD” – means you are calculating the standard deviation of values within that moving window.

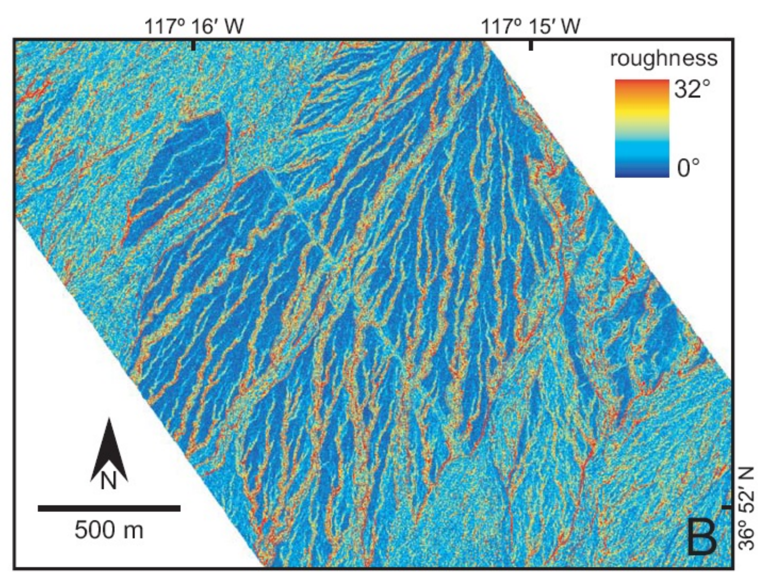

Figure 6. Surface roughness map of the Red Wall Canyon alluvial fan in northern Death Valley. Surface roughness is calculated as the standard deviation of slope in a 3 cell x 3 cell moving window. Modified from Frankel and Dolan (2007).

Optional: Slope Aspect Maps

Slope aspect maps can also be useful in quantifying fault displacement. This is particularly true in regions with well-developed alluvial fans in strike-slip tectonic settings. Slope aspect map aid in the reconstruction of the fan apex as well as offset channels because they can highlight subtle topographic features by abrupt changes in slope direction (Fig. X). Slope aspect maps can be produced as follows.

1. Enter ArcToolbox
   navigate to 3D Analyst Tools → Raster Surface → Aspect

2. Select your input dataset (Input raster)

3. Define the name for your aspect map

4. Click OK

Note: Slope aspect maps made need to be classified to highlight the slope directions that best define the landform you are interested in. To do this, click on the “Symbology” tab under Layer Properties and select “Classified” on the left. From here you can assign specific values for azimuth directions and ranges to highlight.

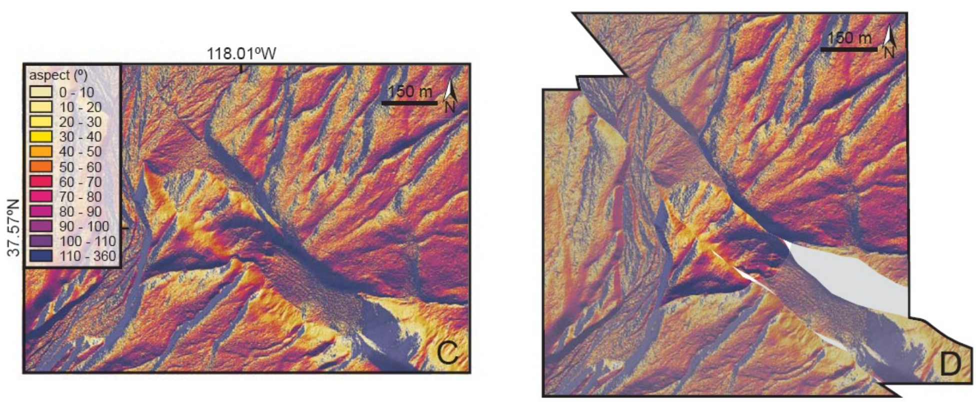

Figure 7. Slope aspect map derived from lidar topographic data for the Furnace Creek alluvial fan in central Fish Lake Valley (location 2 in Figure 1). The slope aspect map aids in the reconstruction of the right-laterally offset fan to quantify fault displacement. After Frankel et al. (2007b).

Quantifying Fault Displacement

This portion of these manual is presented as a complete supplemental on line material for Zielke and Arrowsmith, in preparation. It covers the conceptual as well as practical aspects of manipulating high resolution topography data and measuring strike-slip fault offset—as is found along much of the San Andreas Fault system in California.

In addition, this web site: http://www.public.asu.edu/~ozielke/programs_tools/data/LaDiCaoz_New/index.html has more documentation, sample datasets, and movies which take the users through each step of the DEM data handling and channel offset measurement activity.

References

Arrowsmith, J.R., and O. Zielke, 2009, Tectonic geomorphology of the San Andreas fault zone from high resolution topography: an example from the Cholame segment: Geomorphology, v. 113, p. 70-81, doi:10.1016jgeomorph.2009.01.002.

Brogan, G.E., K.S. Kellog, D.B. Slemmons, and C.L. Terhune (1991), Late Quaternary faulting along the Death-Valley Furnace Creek fault system, California and Nevada: U.S. Geological Survey Bulletin 1991, 23 p.

Bull, W.B., 1977, The alluvial fan environment: Progress in Physical Geography, v. 1, p. 222-270.

Bull, W.B., 1991, Geomorphic responses to climatic change: New York, Oxford University Press, 326 p.

Burchfiel, B.C., and Stewart, J.C., 1966, "Pull-apart" origin of the central segment of Death Valley, California: Geological Society of America Bulletin, v. 77, p. 439-442.

Burchfiel, B.C., Molnar, P., Zhang, P., Deng, Q., Zheng, W., and Wang, Y., 1995, Example of a supradetachment basin within a pull-apart tectonic setting: Mormon Point, Death Valley, California: Basin Research, v. 7, p. 199-214.

Carter, W.E., Shrestha, R.L., and Slatton, K.C., 2007, Geodetic laser scanning: Physics Today v. 60, p. 41-47.

Frankel, K.L., 2007, Fault slip rates, constancy of seismic strain release, and landscape evolution in the eastern California shear zone [Ph.D. dissertation]: Los Angeles, University of Southern California, 179 p.

Frankel, K.L., and Dolan, J.F., 2007, Characterizing arid region alluvial fan surface roughness with airborne laser swath mapping digital topographic data: Journal of Geophysical Research, v. 112, F02025, doi:10.1029/2006JF000644.

Frankel, K.L., Dolan, J.F., Owen, L.A., Finkel, R.C., and Hoeft, J.S., 2007, Spatial variations in slip rate along the Death Valley-Fish Lake Valley fault system from LiDAR topographic data and cosmogenic ^{10}Be geochronology: Geophysical Research Letters, v. 34, doi:10.1029/2007GL030549.

Frankel, K.L., Brantley, K.S, Dolan, J.F., Finkel, R.C., Klinger, R., Knott, J., Machette, M., Owen, L.A., Phillips, F.M., Slate, J.L, and Wernicke, B.P., 2007, Cosmogenic ^{10}Be and ^{36}Cl geochronology of offset alluvial fans along the northern Death Valley fault zone: Implications for transient strain in the eastern California shear zone: Journal of Geophysical Research - Solid Earth, v. 112, doi:10.1029/2006JB004350.

Glenn, N. F., Streuker, D. R., Chadwick, D. J., Thackray, G. D., and Dorsch, S. J., 2006, Analysis of LiDAR-derived topographic information for characterizing and differentiating landslide morphology and activity: Geomorphology, v. 73, p. 131-148.

Hamilton, W., 1988, Detachment faulting in the Death Valley region, California and Nevada: U.S. Geological Survey Bulletin 1790, p. 763-771.

Hudnut, K.W., Borsa, A., Glennie, C., and Minster, J.-B., 2002, High-resolution topography along surface rupture of the 16 October 1999 Hector Mine, Calfornia, earthquake (M_W 7.1) from airborne laser swath mapping: Bulletin of the Seismological Society of America, v. 92, p. 1570-1576.

Klinger, R.E., 2001, Stop A3: Evidence for large dextral offset near Red Wall Canyon, in Quaternary and late Pliocene geology of the Death Valley region: Recent observations on tectonic, stratigraphy, and lake cycles, in Machette, M.N., Johnson, M.L., and Slate, J.L., eds., U.S. Geological Survey Open File Report 01-51, p. A32-A37.

Knott, J.R., Tinsley III, J.C., and Wells, S.G., 2002, Are the benches at Mormon Point, Death Valley, California, USA, scarps or shorelines?: Quaternary Research, v. 58, p. 352-360.

Lawson, A., and H. Reid, 1908, The California Earthquake of April 18, 1906: Report of the State Earthquake Investigation Commission, Carnegie Inst. of Washington, Washington, D. C.

Lowenstein, T.K., Li, J., Brown, C.B., Roberts, S.M., Ku, T.L., Luo, S., and Yang, W., 1999, 200 k.y. paleoclimate record from Death Valley salt core: Geology, v. 27, p. 3-6.

Matmon, A., Nichols, K. and Finkel, R., 2006, Isotopic insights into smoothening of abandoned fan surfaces, Southern California: Quaternary Research, v. 66, p. 109-118.

McKean, J., and Roering, J., 2004, Objective landslide detection and surface morphology mapping using high-resolution airborne laser altimetry: Geomorphology, v. 57, p. 331–351.

Oskin, M.E., Le, K., and Strane, M.D., 2007, Quantifying fault-zone activity in arid environments with high-resolution topography: Geophysical Research Letters, v. 34, doi:10.1029/2007GL031295.

Poage, M.A., and Chamberlin, C.P., 2002, Stable isotopic evidence for a Pre-Middle Miocene rain shadow in the western Basin and Range: Implications for the paleotopography of the Sierra Nevada: Tectonics, v. 21, doi:10.1029/2001TC001303.

Prentice, C.S., C.J. Crosby, C.S. Whitehill, J.R. Arrowsmith, K.P. Furlong, D.A. Phillips, 2009, GeoEarthscope LiDAR illuminates northern California's active faults: Eos, Transactions of the American Geophysical Union, v. 90, p. 55.

Ritter, J. B., et al., 1993, Quaternary evolution of Cedar Creek alluvial fan, Montana: Geomorphology, v. 8, p. 287–304.

Sieh, K. E., 1978, Slip along the San Andreas fault associated with the great 1857 earthquake, *Bull. Seis. Soc. Am.*, *68(5)*, 1421-1448.

Wells, S.G., McFadden, L.D., and Dohrenwend, J.C., 1987, Influence of late Quaternary climatic changes on a desert piedmont, eastern Mojave desert, California: Quaternary Research, v. 27, p. 130-146.

Wernicke, B., Axen, G.J., and Snow, J.K., 1988, Basin and Range extensional tectonics at the latitude of Las Vegas, Nevada: Geological Society of America Bulletin, v. 100, p. 1738-1757.

Zielke, O., Arrowsmith, J.R., Ludwig, L.G., and Akciz, S.O., 2010, Slip in the 1857 and earlier large earthquakes along the Carrizo Plain, San Andreas fault: Science, v. 327, p. 1119-1122.

Zielke, O., and Arrowsmith, J R., in preparation, Supplementary material to "LaDiCaoz and LiDARimager-MATLAB GUIs for LiDAR data handling and lateral displacement measurement".